



Published in final edited form as:

Photochem Photobiol. 2014 September ; 90(5): 1126–1135. doi:10.1111/php.12286.

Combination of Oral Vitamin D₃ with Photodynamic Therapy Enhances Tumor Cell Death in a Murine Model of Cutaneous Squamous Cell Carcinoma

Sanjay Anand^{1,2}, Kishore R. Rollakanti¹, Ronald L. Horst³, Tayyaba Hasan⁴, and Edward V. Maytin^{1,2,4,*}

¹Department of Biomedical Engineering, Cleveland Clinic, Cleveland, OH

²Department of Dermatology, Cleveland Clinic, Cleveland, OH

³Heartland Assays LLC, Ames, IA

⁴Wellman Center for Photomedicine, Harvard Medical School, Boston, MA

Abstract

Photodynamic therapy (PDT), in which 5-ALA (a precursor for protoporphyrin IX, PpIX) is administered prior to exposure to light, is a nonscarring treatment for skin cancers. However, for deep tumors, ALA-PDT is not always effective due to inadequate production of PpIX. We previously developed and reported a combination approach in which the active form of vitamin D₃ (calcitriol) is given systemically prior to PDT to improve PpIX accumulation and to enhance PDT-induced tumor cell death; calcitriol, however, poses a risk of hypercalcemia. Here, we tested a possible strategy to circumvent the problem of hypercalcemia by substituting natural dietary vitamin D₃ (cholecalciferol; D₃) for calcitriol. Oral D₃ supplementation (10 days of a 10-fold elevated D₃ diet) enhanced PpIX levels 3- to 4-fold, and PDT-mediated cell death 20-fold, in subcutaneous A431 tumors. PpIX levels and cell viability in normal tissues were not affected. Hydroxylated metabolic forms of D₃ were only modestly elevated in serum, indicating minimal hypercalcemic risk. These results show that brief oral administration of cholecalciferol can serve as a safe neoadjuvant to ALA-PDT. We suggest a clinical study, using oral vitamin D₃ prior to PDT, should be considered to evaluate this promising new approach to treating human skin cancer.

INTRODUCTION

Nonmelanoma skin cancers (NMSC), including squamous cell carcinoma (SCC) and basal cell carcinoma (BCC), comprise the majority of skin malignancies with an increasing incidence in Caucasian populations worldwide (1,2). Nonmelanoma skin cancers are currently treated by surgical excision, but better alternatives are needed, particularly in the case of patients with multiple and recurring lesions, *e.g.* organ transplant patients. Since surgical excision can result in scars that are hypertrophic and unsightly, Photodynamic

Therapy (PDT) is being considered as a nonscarring and repeatable treatment alternative for NMSCs in dermatologic oncology, particularly for the treatment of carcinomas and precancers (3).

Photodynamic therapy is a combination treatment involving a photosensitizer (PS) and light in the presence of oxygen to kill cancer cells (4,5). Although none of the three components used for PDT are toxic on their own, the activation of PS by light causes the production of reactive oxygen species (ROS), which initiates the tumor cell death (3–5). Photodynamic therapy using 5-aminolevulinic acid (ALA), widely known as ALA-PDT, involves the administration of ALA as a pro-drug that is converted to an intracellular photosensitizer (protoporphyrin IX; PpIX), and is rapidly being accepted as a preferred modality in dermatologic oncology (3,6–9). ALA-PDT offers the advantage of dual selectivity, because both the PpIX and the visible light can be localized to the tumor, minimizing any damage to the normal tissue. In dermatology clinics, ALA-PDT is successfully used for treatment of actinic keratosis (sun-induced precancers) and squamous carcinoma *in situ* (8–12).

However, success rates for normal BCC and invasive SCC remain suboptimal, especially after a single PDT treatment, as compared to the standard mode of care, surgical excision. ALA-PDT is also used for treatment of carcinomas of internal organs such as esophagus, bladder and GU tract (3,9,13). However, ALA-PDT in its current form is ineffective in achieving a cure for deep or relapsing tumors of any origin, due to inefficient ALA uptake and uneven distribution of PpIX.

The importance of three determinants (drug, light and oxygen) for a successful outcome of PDT has been supported by a number of studies providing insights into underlying mechanisms (4, 5, 14–16). While a number of factors, either alone or in combination may limit the outcome of PDT, the failure of the therapy involves a subpopulation of cancer cells that manage to escape from cell death. A recent approach developed in our laboratory is the use of a short-term differentiation therapy in combination with ALA-PDT, a regimen we call combination PDT (cPDT) (3). The cPDT alters the biological response of the target cancer cells, enhancing their susceptibility to ALA-PDT by elevating their PpIX levels and by increasing cell death through additional mechanisms (3). Cancer cells often bypass normal physiological controls on pathways of growth, differentiation and survival to circumvent the cell death and the concept of cPDT is to counteract these abnormalities, using selected small molecule agents. Thus, we found that certain differentiation promoting agents such as methotrexate (MTX) (17,18), vitamin D₃ (12,19,20) and 5-fluorouracil (5-FU) (21), when given prior to ALA-PDT, make cancer cells more susceptible to cell killing through accumulation of higher levels of PpIX. We have successfully tested the cPDT concept in various preclinical models including cultured cells (19,22), 3D organotypic models *in vitro* (18,19) and murine tumor models *in vivo* (3,18,21), using MTX, vitamin D₃, or 5-FU in a 3-day pretreatment regimen.

Vitamin D₃ (referred to here as *vitamin D₃* when used generically, or by individual names of specific chemical forms as described below) is a prohormone with multiple forms, as shown in Fig. 1. The major physiological function of vitamin D₃ in vertebrates is to maintain extracellular fluid concentrations of calcium and phosphorus within a normal range. Vitamin

D₃ physiology and metabolism is quite complex (Fig. 1). Cholecalciferol (D₃), the form usually found in dietary supplements, is normally made in the body from 7-dehydrocholesterol (pro-D₃). Pro-D₃ is converted to pre-D₃ by exposure of skin to the ultraviolet B spectrum (290–315 nm) from sunlight. Pre-D₃ then undergoes thermal isomerization to D₃ (23,24). Cholecalciferol, after binding to carrier proteins (vitamin D-binding protein in particular), is then 25-hydroxylated in the liver to become calcidiol (25-hydroxyvitamin D₃; monohydroxy D₃; MH D₃). 25-hydroxylation is catalyzed by the P450 enzymes CYP27A1 or CYP24R1 (24,25). Calcidiol is then 1-hydroxylated in the kidney and becomes calcitriol (1,25-dihydroxyvitamin D₃; dihydroxy D₃; DH D₃). In addition to renal calcitriol synthesis, there is substantial evidence for extrarenal synthesis of calcitriol in organs like skin and prostate, and also in tumors of different origins (25–27). Calcitriol is the most potent and active hormonal form of D₃ that maintains calcium homeostasis by its actions in bones, kidneys, intestines and parathyroid glands. Calcitriol acts through the D₃ receptor (VDR), which is expressed in a wide variety of cells and tissues including cancer cells. The 24-hydroxylation of calcidiol and calcitriol by 24-hydroxylase (CYP24A1) is the primary mechanism and the first step in the metabolic pathway to degrade these vitamin D metabolites [reviewed in (28–31)]. The nonclassic actions of calcitriol include regulation of cellular proliferation and differentiation, the latter being explored in this study. Although calcitriol is known to inhibit proliferation, it has also been reported to have biphasic effects, *i.e.* at subnanomolar concentrations it promotes proliferation and at higher concentrations inhibits proliferation. Differentiation, on the other hand, is induced under both the conditions (30,32).

In a recently published study, we showed that the active form of D₃ (calcitriol) can stimulate ALA-mediated PpIX accumulation in A431 SCC tumors in mice when administered as a systemic bolus of 1 µg kg⁻¹ day⁻¹ for 3 days, without any adverse effects (20). Although the calcitriol was given for only 3 days prior to PDT, the µg doses employed could theoretically pose a risk for hypercalcemia in the clinical setting (31). To address this issue, in this study we explore the use of the dietary form of vitamin D₃ (cholecalciferol; D₃) as a PDT pretreatment. We hypothesize that cholecalciferol, when given orally, will raise serum (and also tissue) levels of calcidiol and calcitriol, to levels that will be sufficient to exert a PpIX-enhancing effect and augment tumor killing *in vivo* in a safe and effective manner. The goal at the outset of this study was to attempt to establish conditions under which the PpIX-elevating effect of calcitriol can be achieved by transiently increasing the input of its natural precursors, cholecalciferol and calcidiol, prior to the administration of PDT in tumor-bearing mice. We administered D₃ at elevated levels (5X and 10X above normal) in the diet for 10 days, a regimen that does not cause hypercalcemia. Some mice were given systemic calcitriol as a positive control. Data will be presented, showing a significant increase in PpIX levels within tumors and an increase in tumor cell death after ALA-PDT, in mice receiving a high D₃ diet relative to mice on the control diet. Our findings suggest the possibility of using a natural approach to raise calcitriol levels via dietary supplementation, prior to ALA-PDT, thereby avoiding hypercalcemic side effects.

METHODS

Cell culture

A431, a human squamous cell carcinoma cell line, was purchased from Animal Type Culture Collection (ATCC; Manassas, VA) and cultured at 37°C with 5% CO₂ in high-glucose DMEM supplemented with 10% fetal bovine serum and penicillin-streptomycin.

Generation of subcutaneous tumors by injection of A431 cells in nude mice

One million A431 cells diluted in 0.1 mL injection medium (Matrigel; BD Bioscience, San Jose, CA; mixed 1:1 with culture medium) were injected in the flanks of immunocompromised nude mice (Charles River Laboratories, Wilmington, MA). After 8–10 days, visible/palpable nodules at the site of injection were observed.

Differentiation pretreatment regimen using dietary or systemic vitamin D₃

Nude mice injected with A431 cells were switched to AIN-93G diet (Research Diets Inc., New Brunswick, NJ) custom formulated to contain 5000 or 10 000 IU D₃ kg⁻¹ along with normal diet control that contained 1000 IU D₃ kg⁻¹. Mice were fed these diets *ad libitum* for 10 days.

The range of dietary D₃ dosage was based on results published by Kovalenko *et al.* (33). For systemic preconditioning, mice received one of the three different metabolic forms of vit D₃, once a day for 3 days. D₃ (Cholecalciferol, 40 µg kg⁻¹), monohydroxy D₃ (Calcidiol, 25(OH) D₃, 250 µg kg⁻¹) or dihydroxy D₃ (Calcitriol, 1,25(OH)₂D₃, 1 µg kg⁻¹) were injected through the intraperitoneal route, without any visible effects on the health of the mice. The dose of D₃ was similar to that delivered by supplementation with 10 000 IU diet, and the doses for monohydroxy D₃ (34) and dihydroxy D₃ (20) were based on previous studies. On the 11th day for dietary regimen or on the 4th day for the systemic regimen, ALA (200 mg kg⁻¹) was given intraperitoneally for 4 h. At this time, mice were either sacrificed for tumor and skin harvest or tumors were exposed to light for PDT through the skin. To observe the tumor specificity of the differentiation therapy on cell killing post-PDT, skin away from tumor was also exposed to the same dose of light and tumor and skin samples harvested at 24 h post-PDT.

Light exposure for PDT

Photodynamic therapy was performed by exposing tumors or skin to the red light (633 nm) using a noncoherent light source (LumaCare Products, Newport Beach, CA) at a fluence of 100 J cm⁻². The light source was calibrated using a FieldMate laser power meter (Coherent, Santa Clara, CA).

Analysis of PpIX fluorescence and histologic markers of differentiation, proliferation and cell death in A431 tumors

A431 tumors from nude mice were harvested, embedded in OCT, sectioned (10 µm) using a cryotome (Leica Microsystems, Buffalo Grove, IL) and analyzed on a confocal microscope (Leica Microsystems) as described previously (20). For histological analysis, tumors and skin samples were formalin fixed, paraffin embedded and sectioned (5 µm) using a

microtome (Leica Microsystems). Standard hematoxylin and eosin (H&E) staining, immunohistochemical staining (E-Cad & Ki67) and cell death analysis by TUNEL assay were performed exactly as described previously (20). Specific fluorescence from digital images was quantitated using IP Lab image processing software (Spectra Services, Ontario, NY), as described (18). Cell death in A431 tumors was quantitated using high power images of H&E-stained sections. Three different observers (SA, KR & EVM) independently scored each of three different criteria, *i.e.* hypochromicity, pyknotic nuclei and the presence of dead (open) areas, on a scale of 1–9 for each tumor image. See Fig. 6 legend for further details.

UVB source and exposure protocol

Ultraviolet B (UVB) light was delivered from a bank of UV bulbs (RPR-3000A, Southern New England Ultraviolet, Branford, CT). The percentage of the total irradiance in the UVA, UVB and UVC range was 16%, 74% and 10%, respectively. Thus, three-fourths of the light output was in the UVB range. The UVC component was removed with a UVC filter (Kodacel, Kodak, Rochester, NY). Exposure times for proper dose delivery were determined by measuring energy output with a power meter (IL-1700, International Lights, Newburyport, MA). Nude mice with A431 tumors were exposed to the UV light (24 mJ cm^{-2} ; fluence rate $0.8 \text{ mJ cm}^{-2} \text{ s}^{-1}$) once daily for 3 days (on days 8–10 of the dietary supplementation regimen), followed by harvest of tumor and skin on day 11. Tumors were processed for PpIX analysis, and skin samples were stained for TUNEL to observe cell death post-UVB, as described above. The dose of UV used here was based on our previous study involving UVB exposure of human and murine skin (35).

Measurement of vitamin D₃ metabolic forms in serum

Mice were euthanized and blood was collected by cardiac puncture, followed by clotting at room temperature for 15 min and centrifugation at 3000 rpm for 5 min. Supernatant serum was shipped on dry ice for determination of vitamin D₃ and vitamin D₃ metabolite levels at Heartland Assays (Ames, IA).

Statistics

Two-sample t tests were used to analyze differences between treated and untreated control groups, using Microsoft Excel. A value of $P < 0.05$ was considered statistically significant. Details of sample size and method of analysis are provided in the figure legends.

RESULTS AND DISCUSSION

Dietary supplementation with vitamin D₃ enhances the production of PpIX in A431 subcutaneous tumors in nude mice

To study how dietary supplementation with vitamin D₃ affects PpIX levels in SCC tumors, A431 cells were implanted in nude mice (Fig. 2a). Mice were then switched to a D₃-supplemented diet (either 5000 or 10 000 IU kg⁻¹ D₃ in the chow), or fed with a normal diet (1000 IU kg⁻¹) for 10 days. The elevated diets were based on results from a previous study (33), and represent two different elevated dietary regimes (five times the normal level, “5 K”; or 10 times the normal level, “10 K”). The active form of vitamin D₃ (calcitriol, $1 \mu\text{g kg}^{-1} \text{ day}^{-1}$) that worked previously in this A431 tumor model (20) was used as a positive

control in parallel with the dietary supplementation experiments. Mice on the D₃-supplemented diets showed elevated levels of PpIX in tumors as compared to similar tumors from mice on a normal diet (Fig. 2b).

Specifically, confocal images showed a relatively elevated and more uniform distribution of PpIX in tumors from mice supplemented with either the 5 K or 10 K D₃ diet (Fig. 2b). Mice receiving systemically administered calcitriol, as a positive control, showed a robust PpIX induction, as expected (Fig. 2b), a relative induction of 3.5-fold when the PpIX-specific fluorescence from digital confocal micrographs was analyzed by Image Processing software (Fig. 2c). Interestingly, PpIX levels after pretreatment with the 5 K and 10 K supplemented diets were increased 2.5-fold and three-fold, respectively, a change that was highly significant in each case (Fig. 2c).

The serum levels of D₃ and its mono- and dihydroxylated metabolic forms were assayed from serum samples isolated from mice fed with the normal diet or with the D₃-supplemented diet containing 5 or 10 times the normal D₃ amount. As expected, dietary supplementation with D₃ elevated the serum levels of D₃, calcidiol and calcitriol by approximately 2- to 3-fold as compared to their corresponding serum levels in mice fed with the normal diet (Table 1). Serum levels of calcitriol (the most active hormonal form) achieved by 5X or 10X supplementation with D₃ appeared identical to levels achieved after systemic calcitriol injection (Table 1).

The level of PpIX in tumor cells is a critical determinant of the cell killing induced by ALA-PDT, and the results described here demonstrate that oral D₃ (cholecalciferol) when given as a 5 or 10 times dietary supplement elevates the levels of PpIX in A431 tumors, essentially bypassing the risk of inducing hypercalcemia. The latter statement is based on extensive data from several investigators. For example, Fleet *et al.* showed that mice ingesting a diet supplemented with 20 000 IU kg⁻¹ of D₃, for up to 7 weeks, remained normocalcemic (36). In another study that reported vitamin D₃ growth-inhibitory effects in nude mice bearing orthotopic breast or prostate tumors, the mice ingested a 5000 IU kg⁻¹ diet for 4 weeks or received systemic calcitriol (0.1 μg per mouse, equivalent to ~4 μg kg⁻¹). A statistically significant increase in serum calcium (~10%) was recorded in the mice receiving systemic calcitriol, whereas calcium levels remained unchanged in mice on the high D₃ diet (27).

Of relevance here, the mechanism underlying vitamin D₃- mediated enhancement of PpIX levels has been elucidated in two recently published studies (20,37). Preferential upregulation of coproporphyrinogen oxidase (CPO) and down regulation of ferrochelatase (FC) levels, two key enzymes upstream and downstream of PpIX, respectively, was observed in A431 tumors treated with calcitriol as a pretreatment regimen (20). The differentiation-inducing pretreatment was also shown to regulate CPO expression through upregulation of the CPO gene promoter by transcription factors called CCAAT enhancer binding proteins (C/EBPs) (37).

Systemic preconditioning using vitamin D₃ metabolites enhances PpIX accumulation in A431 tumors

The physiological effects of D₃, after dietary intake or after natural conversion from 7-dehydrocholesterol by exposure to sunlight, relies on hydroxylation of D₃ to calcidiol in liver and subsequently to calcitriol in kidney by specific enzymes carrying out these steps (Fig. 1). To compare the effects of dietary supplementation to effects resulting from direct systemic administration of D₃ or its hydroxylated metabolic forms, mice bearing A431 tumors were given D₃, calcidiol or calcitriol by systemic injection, once daily, for 3 days. On day 4, ALA was systemically administered for 4 h, and tumors harvested for PpIX analysis by confocal microscopy. Pretreatment with systemic D₃ or its hydroxylated forms resulted in an increase in PpIX accumulation throughout the tumor, as compared to tumors from mice that receiving vehicle (PBS) only (Fig. 3a). Quantitation of PpIX from confocal fluorescence images showed a gradual increase in PpIX levels related to the state of hydroxylation of D₃ (Fig. 3b). As compared to vehicle, D₃ and monohydroxy D₃ showed approximately 2.5- and 3-fold increase, respectively, whereas tumors receiving dihydroxy D₃ showed approximately 3.5-fold increase in PpIX levels as compared to vehicle control (Fig. 3b).

Under these conditions, the serum levels of calcidiol and calcitriol were considerably elevated (3- to 5-fold) after systemic administration of D₃ or of calcidiol (Table 1). Injections of calcitriol itself, however, resulted in only a two-fold elevation of calcitriol suggesting activation of feedback inhibition of calcitriol production as outlined in Fig. 1.

It was notable that supplementation of D₃ by either an oral route (Fig. 2c) or systemic route (Fig. 3b) had a similar effect on PpIX levels of A431 tumors. This further supports our hypothesis that oral vitamin D₃ supplementation may be an effective and safer alternative to systemic administration of calcitriol as a combination agent for PDT (20).

Physiologically, there are two ways to achieve adequate levels of vitamin D₃: (i) dietary ingestion of D₃ (cholecalciferol), or (ii) exposure to the UVB component of sunlight, which catalyzes the synthesis of D₃ from its precursor, 7-dehydrocholesterol. Subsequent hydroxylation steps in the liver to make calcidiol, and then in the kidney to make calcitriol, are subject to physiological regulation (24,29). We explored the possibility of using short-term low-dose exposure to UVB as a neoadjuvant therapy to enhance the PpIX levels in the A431 tumors. Nude mice bearing A431 tumors, fed on either a normal or 10 K D₃ diet, were exposed to 24 mJ cm⁻² UVB, once a day for 3 days to induce the conversion of 7-dehydrocholesterol to cholecalciferol. A significant increase (~3-fold) in PpIX levels in tumors from mice on a normal diet that received UVB exposure was observed, relative to no UVB exposure (Fig. 3c). In the group of mice receiving a 10 K diet, UVB exposure led to only a slight increase in PpIX levels that were not statistically significant. The 10 K diet alone resulted in a four-fold increase in PpIX levels, therefore, any further increase due to UVB exposure seems to be physiologically irrelevant and may reflect the influence of feedback inhibition mechanisms that limit the amount of conversion of pre-D₃ to D₃ in the skin (38).

Both dietary and systemic preconditioning with vitamin D₃ induces cellular differentiation and proliferation in A431 tumors

Vitamin D₃, directly or indirectly, regulates expression of genes that control cell cycle, proliferation, differentiation, apoptosis, angiogenesis and carcinogenesis in a wide range of tissues and organs (23, 24, 39, 40). To analyze the effect of dietary or systemic manipulation of vitamin D₃ levels in mice with A431 tumors, we examined markers of differentiation (E-cadherin) and proliferation (Ki67) using immunohistochemistry. Dietary supplementation of D₃ resulted in increased expression of E-cadherin in A431 tumors (Fig. 4a, left panel). Quantitation of E-cadherin-specific fluorescence showed a gradual increase in differentiation with respect to the dose of Vit D₃ in the supplemented diet. The 5 K diet showed a ~2-fold increase, whereas the 10 K diet showed a three-fold increase in E-cadherin expression. As expected, calcitriol had the maximum effect with a ~3.5-fold increase in the E-cadherin levels (Fig. 4b, left graph). Dietary supplementation with Vit D₃ also caused increased proliferation in A431 tumors, as shown by elevated Ki67 expression levels in Vit D₃-supplemented tumors as compared to normal diet controls (Fig. 4a, right panel). Quantitation of Ki67-specific fluorescence showed a four- and eight-fold increase in expression for 5 K and 10 K diets, respectively. As observed previously, the calcitriol-treated tumors had a maximal 11-fold increase in Ki67 levels as compared to normal diet controls (Fig. 4b, right graph).

The effects that systemic administration of several vitamin D₃ metabolic forms exerts upon A431 tumors appear to be similar to those of dietary supplementation. Increased E-cadherin expression was observed in tumors receiving various metabolic forms of vitamin D₃, relative to vehicle (PBS) controls (Fig. 4c, left panel). E-cadherin-specific fluorescence showed a ~2-fold increase in the cases of D₃ and calcidiol (MH D₃) (Fig. 4d, left graph). As expected, calcitriol had the most profound effect among the metabolic forms, with E-cadherin increasing 3.5-fold over vehicle control (Fig. 4d, left graph). Effects on proliferation were also similar when comparing systemic with dietary supplementation. Ki67 levels were elevated in tumors receiving each of the vitamin D₃ metabolic forms (Fig. 4c, right panel). Quantitation of Ki67 expression levels showed a six- and eight-fold increase for D₃ and calcidiol, respectively, whereas calcitriol exerted a 10.5-fold increase (Fig. 4d, right graph).

The systemic delivery of D₃ or its mono- and dihydroxylated forms, while an artificial situation here (not intended for therapeutic utility), was nonetheless informative and assures us that the effects of all metabolic conversion pathways between the various metabolites are positive, *i.e.* all intermediates appear to result in the elevation of PpIX in tumors, regardless of the route of delivery. The positive correlation between PpIX levels and the differentiation state of tumor cells was previously seen with other combination agents that enhance PDT, including MTX and 5-fluorouracil (3). On the other hand, the stimulatory effect upon proliferation may be unique to vitamin D₃. While stimulation of cancer cell division sounds like an undesirable thing at first glance, the fact that dividing cells are often more susceptible to damage from radiation-induced effects actually appears to be advantageous for PDT cell killing (see below).

The simultaneous increase in differentiation and proliferation by D₃ observed here is a nonclassical biphasic effect, but it has in fact been observed previously. At low concentrations (subnanomolar range), D₃ acts as a proliferative agent, whereas growth inhibitory properties are displayed at relatively higher concentrations (micromolar range); this is well documented in the literature for many normal and cancer cell lines. Differentiation, on the other hand, is induced at both the nano- and micromolar concentrations (30,32).

PDT-induced cell death is enhanced to similar levels by dietary or systemic preconditioning with vitamin D₃

Increased levels of PpIX in A431 tumors after differentiation pretreatment, either by dietary or systemic supplementation, are meaningful only if the increase results in enhanced cell death after ALA-PDT. Mice bearing A431 tumors were placed on a 10 K diet for 10 days or given systemic calcitriol for 3 days in parallel with normal diet control mice. On day 11, mice received ALA (4 h) followed by PDT. Cell death in harvested tumors was measured 24 h post-PDT. Analysis of dying nuclei (TUNEL labeling) is shown in Fig. 5. Morphometric analysis of hematoxylin and eosin (H&E)-stained tumor sections revealing gross morphological cell death features, including the presence of pyknotic nuclei, loss of intact cells within tumors and loss of staining intensity (hypochromicity) that reflects a lack of proteinsynthetic activity in cells is presented in Fig. 6. Quantitation of TUNEL-positive nuclei/field (Fig. 5a) showed an approximately 20-fold increase in cell death in D₃-treated tumors as compared to those receiving ALA-PDT only (Fig. 5b). Note that dietary and systemic vitamin D₃ pretreatments had similar effects on the level of cell death in A431 tumors (Fig. 5b). To check whether the effects of D₃ preconditioning are tumor specific, normal skin located away from the tumor on the same mouse was exposed to light, and the skin harvested at 24 h post-PDT along with tumor. As seen in Fig. 5c, no significant differences in TUNEL-positive nuclei in normal skin from D₃ - or vehicle-treated mice were seen. In fact, the epidermal layer was completely negative for apoptotic nuclei, except for a few cells in the outermost layer (the stratum corneum); this was similar among all skin samples that received PDT (Fig. 5c).

Cell death-promoting effects of D₃ combined with PDT could also be discerned in H&E-stained A431 tumor sections. As compared to untreated controls, loss of overall staining (hypochromicity) and appearance of dead empty spaces (hypocellularity) was observed in low power images of tumors receiving ALA-PDT (Fig. 6a, top and middle images). The D₃ pretreatment further increased the cell death response as reflected by further loss of cellularity in the tumors receiving a 10 K diet prior to ALA-PDT (Fig. 6a, bottom image). Using three cell death criteria (hypocellularity, pyknotic nuclei and dead/empty space, on a scale of 1–9) to rate a series of high power images from the tumors, we were able to describe the severity of PDT-induced damage on a semiquantitative scale (severity index, Fig. 6c). Vehicle control tumors showed normal staining and were almost devoid of pyknotic nuclei and dead spaces, corresponding to a severity index of 1 (Fig. 6b, top row). At the other end of the scale, tumors with maximal change after treatments showed loss of H&E staining, higher number of shrunken (pyknotic) nuclei and large open areas without cells; the maximum severity index within each category is 9 (Fig. 6b, bottom row). Quantitation of the

three different criteria showed a clear pattern of increase in cell death induced by ALA-PDT, with a further increase for PDT when combined with dietary or systemic vitamin D₃ pretreatment (Fig. 6c).

Mechanisms underlying the enhancement of PDT-induced cell death observed in vitamin D₃-treated tumors were explored in a previous study (20). We have shown the involvement of the extrinsic apoptotic pathway, evident from increased expression of TNF α and caspase-8 in calcitriol-treated A431 tumors (20). A calcitriol-induced increase and localization of TNF α to blood vessels in A431 tumors was also observed, and may represent another underlying mechanism for the large differences observed in PDT-induced cell death after vitamin D₃ pretreatment (20).

CONCLUSIONS

The treatment of nonmelanoma skin cancer by PDT, although approved in European countries, is still less effective on a pretreatment basis than surgical excision. We have shown previously that a combination (cPDT) approach using hormonally active vitamin D₃ (calcitriol) can improve this suboptimal PDT response, but carries at least a theoretical risk of hypercalcemia. In this study, we have shown that preconditioning SCC tumors in mice using the dietary (natural) form of vitamin D₃ leads to a uniform increase in PpIX production and accumulation in the tumors, and results in a significant enhancement of tumor cell death following PDT. Extrapolating from this preclinical study in mice, we suggest that a clinical study involving oral cholecalciferol as a pretreatment before PDT for human patients is a promising approach for an effective new treatment of NMSC. Importantly, compared to calcitriol, the combination of a routine dietary D₃ supplement with PDT should improve patient safety and reduce the regulatory hurdles to overcome when contemplating clinical trials.

Acknowledgments

This work was supported by the National Cancer Institute/NIH grant P01-CA84203 (TH and EVM).

References

1. Rogers HW, Weinstock MA, Harris AR, Hinckley MR, Feldman SR, Fleischer B, Coldiron BM. Incidence estimate of nonmelanoma skin cancer in the United States, 2006. *Arch Dermatol*. 2010; 146:283–287. [PubMed: 20231499]
2. Donaldson MR, Coldiron BM. No end in sight: the skin cancer epidemic continues. *Semin Cutan Med Surg*. 2011; 30:3–5. [PubMed: 21540015]
3. Anand S, Ortel BJ, Pereira SP, Hasan T, Maytin EV. Biomodulatory approaches to photodynamic therapy for solid tumors. *Cancer Lett*. 2012; 326:8–16. [PubMed: 22842096]
4. Hasan, T.; Ortel, B.; Solban, N.; Pogue, BW. Photodynamic therapy of cancer. In: Kufe, D.; Bast, R.; Hait, W.; Hong, W.; Pollock, R.; Weichselbaum, R.; Holland, J.; Frei, E., editors. *Cancer Medicine*. 7. BC Decker, Inc; Hamilton, ON: 2006. p. 537-548.
5. Ortel B, Shea CR, Calzavara-Pinton P. Molecular mechanisms of photodynamic therapy. *Front Biosci*. 2009; 14:4157–4172.
6. Kennedy JC, Pottier RH, Pross DC. Photodynamic therapy with endogenous protoporphyrin IX: basic principles and present clinical experience. *J Photochem Photobiol, B*. 1990; 6:143–148. [PubMed: 2121931]

7. Kennedy JC, Pottier RH. Endogenous protoporphyrin IX, a clinically useful photosensitizer for photodynamic therapy. *J Photochem Photobiol B*. 1992; 14:275–292. [PubMed: 1403373]
8. Kalka K, Merk H, Mukhtar H. Photodynamic therapy in dermatology. *J Am Acad Dermatol*. 2000; 42:389–413. quiz 414–386. [PubMed: 10688709]
9. Zhao B, He YY. Recent advances in the prevention and treatment of skin cancer using photodynamic therapy. *Expert Rev Anticancer Ther*. 2010; 10:1797–1809. [PubMed: 21080805]
10. Fayer D, Corbett M, Heirs M, Fox D, Eastwood A. A systematic review of photodynamic therapy in the treatment of precancerous skin conditions, Barrett's oesophagus and cancers of the biliary tract, brain, head and neck, lung, oesophagus and skin. *Health Technol Assess*. 2010; 14:1–288. [PubMed: 20663420]
11. Jeremic G, Moore CC, Brandt MG, Doyle PC. Neoadjuvant use of photodynamic therapy in Basal cell and squamous cell carcinomas of the face. *ISRN Dermatol*. 2011; 2011:809409. [PubMed: 22363859]
12. Maytin EV, Honari G, Khachemoune A, Taylor CR, Ortel B, Pogue BW, Sznycer-Taub N, Hasan T. Vitamin D Combined with Aminolevulinic Acid (ALA)-Mediated Photodynamic Therapy (PDT) for Human Psoriasis: a Proof-of-Principle Study. *Isr J Chem*. 2012; 52:767–775. [PubMed: 23264699]
13. Dolmans DE, Fukumura D, Jain RK. Photodynamic therapy for cancer. *Nat Rev Cancer*. 2003; 3:380–387. [PubMed: 12724736]
14. Celli JP, Spring BQ, Rizvi I, Evans CL, Samkoe KS, Verma S, Pogue BW, Hasan T. Imaging and photodynamic therapy: mechanisms, monitoring, and optimization. *Chem Rev*. 2010; 110:2795–2838. [PubMed: 20353192]
15. Pogue BW, Samkoe KS, Gibbs-Strauss SL, Davis SC. Fluorescent molecular imaging and dosimetry tools in photodynamic therapy. *Methods Mol Biol*. 2010; 635:207–222. [PubMed: 20552350]
16. Agostinis P, Berg K, Cengel KA, Foster TH, Girotti AW, Gollnick SO, Hahn SM, Hamblin MR, Juzeniene A, Kessel D, Korbelik M, Moan J, Mroz P, Nowis D, Piette J, Wilson BC, Golab J. Photodynamic therapy of cancer: an update. *CA Cancer J Clin*. 2011; 61:250–281. [PubMed: 21617154]
17. Sinha AK, Anand S, Ortel BJ, Chang Y, Mai Z, Hasan T, Maytin EV. Methotrexate used in combination with aminolaevulinic acid for photodynamic killing of prostate cancer cells. *Br J Cancer*. 2006; 95:485–495. [PubMed: 16868543]
18. Anand S, Honari G, Hasan T, Elson P, Maytin EV. Low-dose methotrexate enhances aminolevulinic acid-based photodynamic therapy in skin carcinoma cells in vitro and in vivo. *Clin Cancer Res*. 2009; 15:3333–3343. [PubMed: 19447864]
19. Sato N, Moore BW, Keevey S, Drazba JA, Hasan T, Maytin EV. Vitamin D enhances ALA-induced protoporphyrin IX production and photodynamic cell death in 3-D organotypic cultures of keratinocytes. *J Invest Dermatol*. 2007; 127:925–934. [PubMed: 17068479]
20. Anand S, Wilson C, Hasan T, Maytin EV. Vitamin D₃ enhances the apoptotic response of epithelial tumors to aminolevulinic acid-based photodynamic therapy. *Cancer Res*. 2011; 71:6040–6050. [PubMed: 21807844]
21. Maytin, E.; Anand, S.; Wilson, C.; Iyer, K. 5-Fluorouracil as an Enhancer of Aminolevulinic Acid-Based Photodynamic Therapy for Skin Cancer: New use for a Venerable Agent?. In: Kessel, D.; Hasan, T., editors. *Proc SPIE*. Vol. 7886. 2011. p. OK1-OK8.
22. Ortel B, Sharlin D, O'Donnell D, Sinha AK, Maytin EV, Hasan T. Differentiation enhances aminolevulinic acid-dependent photodynamic treatment of LNCaP prostate cancer cells. *Br J Cancer*. 2002; 87:1321–1327. [PubMed: 12439724]
23. Holick MF. Vitamin D deficiency. *N Engl J Med*. 2007; 357:266–281. [PubMed: 17634462]
24. Bikle, DD., editor. *Vitamin D: Production, Metabolism and Mechanisms of Action*, version of 7/30/2009. MDTEXT.COM Inc; South Dartmouth, MA: 2009.
25. Lehmann B, Meurer M. Vitamin D metabolism. *Derma-tol Ther*. 2010; 23:2–12.
26. Henison, M.; Adams, JS. External 1alpha-hydroxylase. In: Feldman, D.; Pike, JW.; Adams, JS., editors. *Vitamin D*. 3. Elsevier Academic Press; Waltham, MA: 2011. p. 777–806.

27. Swami S, Krishnan AV, Wang JY, Jensen K, Horst R, Albertelli MA, Feldman D. Dietary vitamin D(3) and 1,25-dihydroxyvitamin D(3) (calcitriol) exhibit equivalent anticancer activity in mouse xenograft models of breast and prostate cancer. *Endocrinology*. 2012; 153:2576–2587.
28. Horst, RL. Vitamin D metabolism. In: Feldman, D.; Pike, JW.; Glorieux, FH., editors. *Vitamin D*. 2. Elsevier Academic Press; Waltham, MA: 2005. p. 15-36.
29. Holick, MF. Photobiology of Vitamin D. In: Feldman, D.; Pike, JW.; Glorieux, FH., editors. *Vitamin D*. 2. Elsevier Academic Press; Waltham, MA: 2005. p. 37-45.
30. Bikle, DD. Vitamin D: Role in skin and hair. In: Feldman, D.; Pike, JW.; Glorieux, FH., editors. *Vitamin D*. 2. Elsevier Academic Press; Waltham, MA: 2005. p. 609-630.
31. Krishnan AV, Trump DL, Johnson CS, Feldman D. The role of vitamin D in cancer prevention and treatment. *Endocrinol Metab Clin North Am*. 2010; 39:401–418. [PubMed: 20511060]
32. van Leeuwen, JPTM.; Pols, HAP. Vitamin D: Cancer and differentiation. In: Feldman, D.; Pike, JW.; Glorieux, FH., editors. *Vitamin D*. 2. Elsevier Academic Press; Waltham, MA: 2005. p. 1571-1597.
33. Kovalenko PL, Zhang Z, Yu JG, Li Y, Clinton SK, Fleet JC. Dietary vitamin D and vitamin D receptor level modulate epithelial cell proliferation and apoptosis in the prostate. *Cancer Prev Res*. 2011; 4:1617–1625.
34. Vieth R, McCarten K, Norwich KH. Role of 25-hydroxyvitamin D₃ dose in determining rat 1,25-dihydroxyvitamin D₃ production. *Am J Physiol*. 1990; 258:E780–E789. [PubMed: 2185661]
35. Anand S, Chakrabarti E, Kawamura H, Taylor CR, Maytin EV. Ultraviolet light (UVB and UVA) induces the damage-responsive transcription factor CHOP/gadd153 in murine and human epidermis: evidence for a mechanism specific to intact skin. *J Invest Dermatol*. 2005; 125:323–333. [PubMed: 16098044]
36. Fleet JC, Gliniak C, Zhang Z, Xue Y, Smith KB, McCreedy R, Adedokun SA. Serum metabolite profiles and target tissue gene expression define the effect of cholecalciferol intake on calcium metabolism in rats and mice. *J Nutr*. 2008; 138:1114–1120. [PubMed: 18492843]
37. Anand S, Hasan T, Maytin EV. Mechanism of differentiation-enhanced photodynamic therapy for cancer: upregulation of coproporphyrinogen oxidase by C/EBP transcription factors. *Mol Cancer Ther*. 2013; 12:1638–1650. [PubMed: 23686770]
38. Webb AR, DeCosta BR, Holick MF. Sunlight regulates the cutaneous production of vitamin D₃ by causing its photodegradation. *J Clin Endocrinol Metab*. 1989; 68:882–887. [PubMed: 2541158]
39. Studzinski, GP.; Gocek, E.; Danilenko, M. Vitamin D: Effects on differentiation and cell cycle. In: Feldman, D.; Pike, JW.; Adams, JS., editors. *Vitamin D*. 3. Elsevier Academic Press; Waltham, MA: 2011. p. 1625-1656.
40. Trump, DL.; Johnson, CS. The anti-tumor effects of Vitamin D in other cancers. In: Feldman, D.; Pike, JW.; Adams, JS., editors. *Vitamin D*. 3. Elsevier Academic Press; 2011. p. 1763-1776.

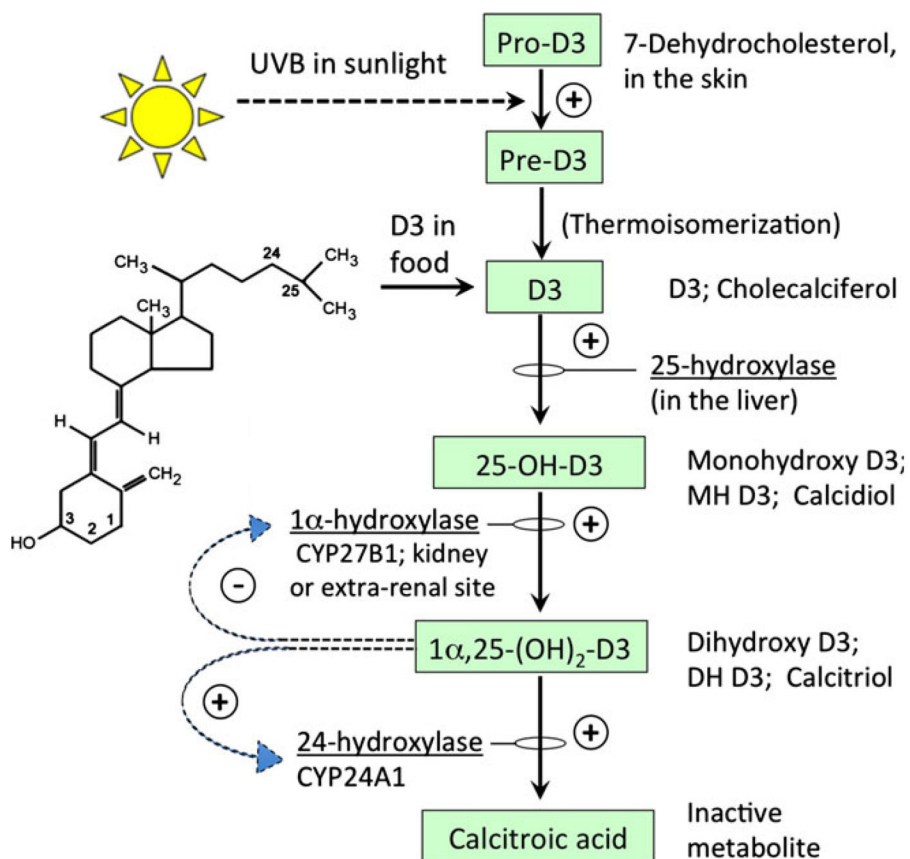


Figure 1. Metabolic pathway for vitamin D₃ synthesis in mammals. Cholecalciferol (D₃), its precursor (Pre-D₃), and its downstream metabolites are shown within boxes. Enzymes that regulate each step are noted, and feedback regulation is indicated by the curved arrows [see references (28–30) for details].

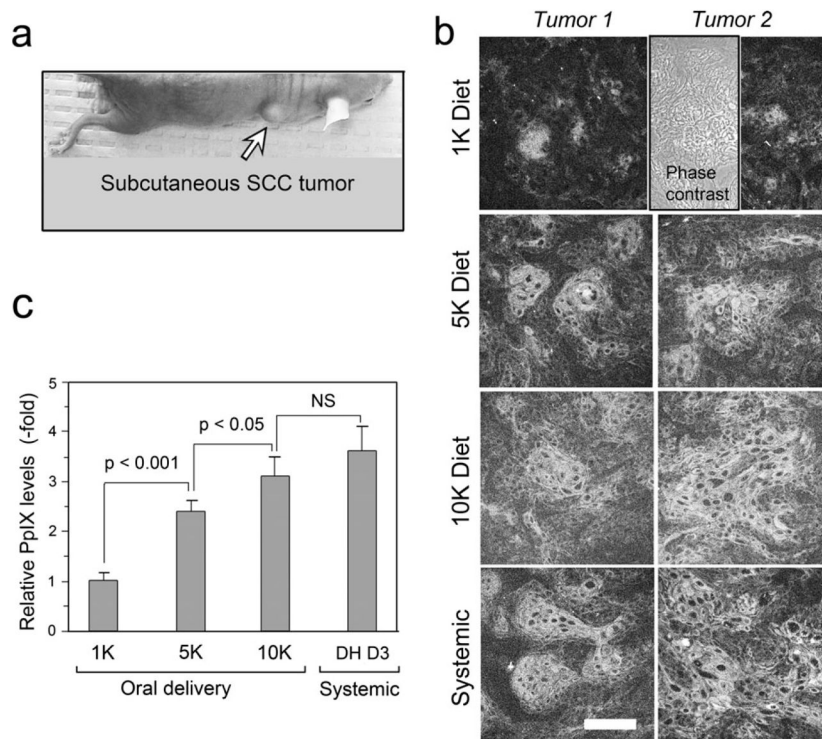


Figure 2. Analysis of PpIX levels in the murine A431 tumor model. (a), Photograph of A431 subcutaneous tumor on a nude mouse. (b), Examples of confocal images, showing PpIX in tumors either after 10 days of dietary pretreatment with a D₃-supplemented diet (5 K or 10 K), or after a normal control diet (1 K), followed by 4 h of systemic ALA to induce PpIX synthesis. *Systemic*, a positive control in which calcitriol (1,25(OH)₂-D₃; dihydroxy-D₃; DH D₃) was given by i.p. injection at 1 μg kg⁻¹ dose for 3 days, followed by ALA. *Phase*, A matching phase contrast image is shown in a representative panel to exhibit the tumor morphology. (c), Quantitation of PpIX-specific fluorescence from digital images using IPLab software (see Methods). Mean ± SEM from 8–10 tumors per treatment group, three images per tumor, is shown. *P* values from an unpaired two-sided Student's *t*-test are shown above the brackets. *NS*, not significant. *Scale bar*, 50 μm.

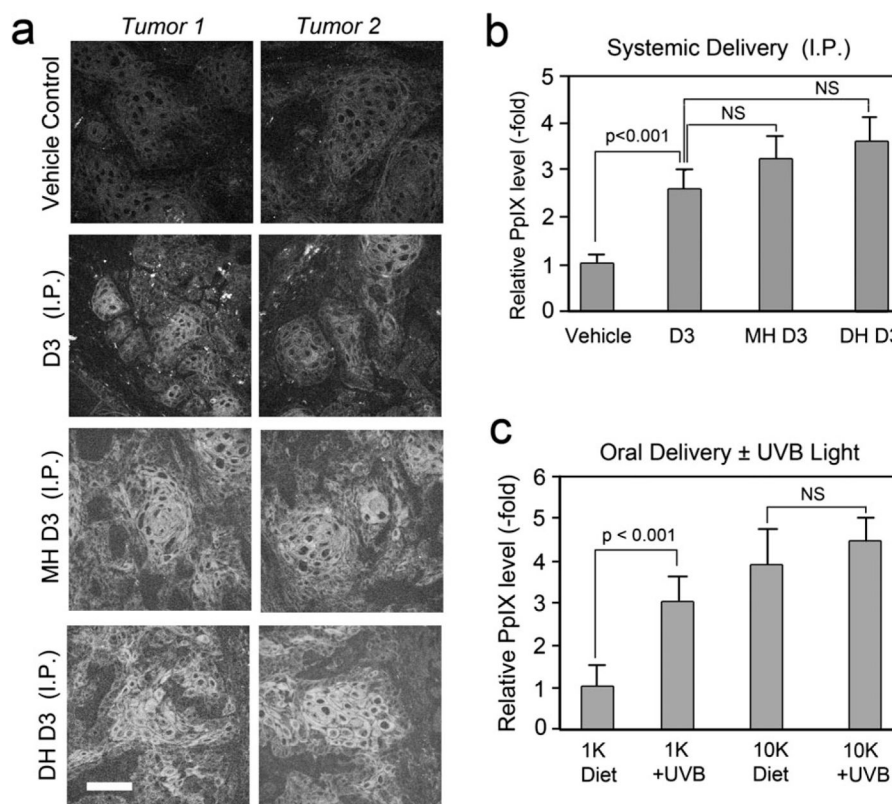


Figure 3. Effect of different metabolic forms of D₃, and of UVB exposure, upon PpIX levels in tumors. (a), Confocal images showing PpIX levels in A431 tumors after 3 days of systemic pretreatment with D₃, monohydroxy-D₃ (MH D₃), dihydroxy-D₃ (DH D₃), or saline as a vehicle control (i.p. delivery) followed by 4 h of ALA. Scale bar 50 μm. (b), Quantitation of PpIX-specific fluorescence after systemic D₃ analogs. Digital images were analyzed using IPLab software; mean ± SEM from three images from each of 4–8 tumors per treatment group. (c), Quantitation of PpIX with/without UVB irradiation. Mice with A431 tumors were fed a Vit D₃ supplemented (10 K) or a normal (1 K) diet, and then exposed to low-dose UVB radiation to induce D₃ synthesis (see Methods for details). Mean ± SEM of three images from each of three to four tumors per treatment group is shown. In both graphs, *P* values from unpaired two-sided *t*-test are shown above the brackets.

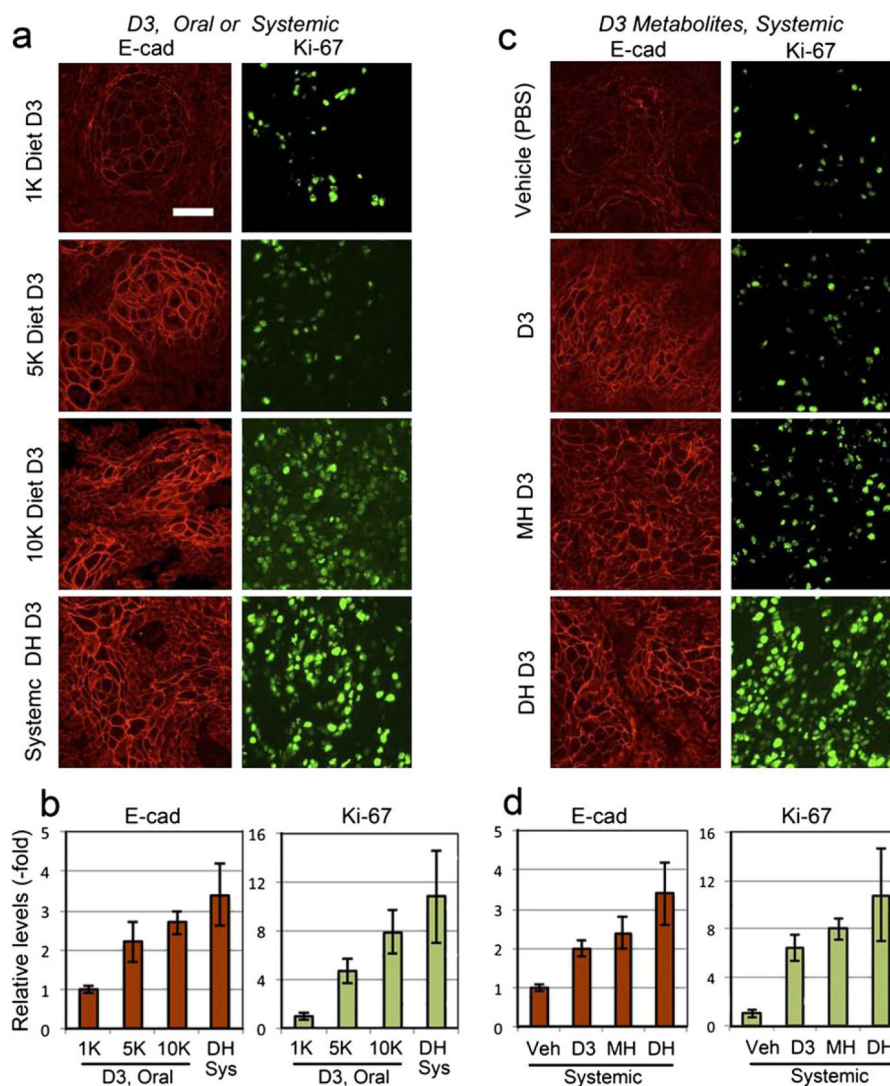


Figure 4. Physiological differentiation and proliferation responses to D₃ preconditioning in A431 tumors. (a, c) Images of paraffin sections from A431 tumors, immunostained with antibodies to: a differentiation marker, *E-cadherin* (E-Cad), or a proliferation marker, *Ki-67*, following dietary and systemic supplementation with D₃ or its metabolites. (b, d), Fluorescence from the secondary antibody probe was quantified in the corresponding graphs shown beneath the immunostained panels; mean \pm SEM from three images from each of three to four tumors per treatment group. Scale bar 50 μ m.

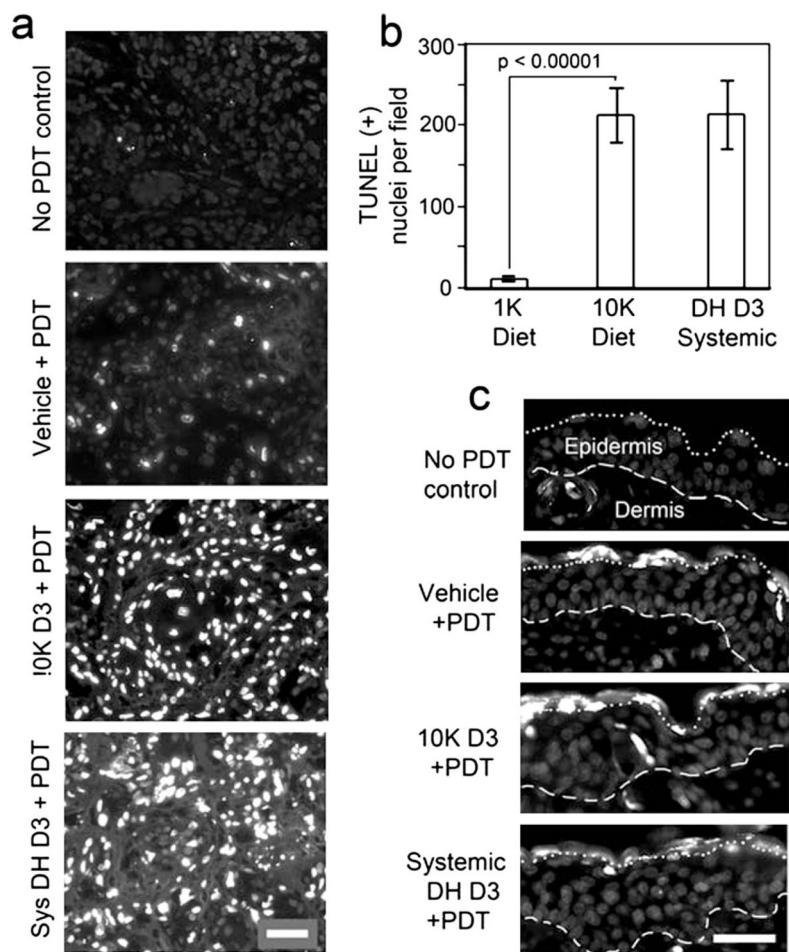


Figure 5. Photodynamic therapy (PDT)-induced cell death is preferentially enhanced by D₃ pretreatment in A431 tumors. (a), TUNEL labeling of apoptotic nuclei at 24 h after PDT exposure (100 J cm^{-2}) is enhanced by pretreatment with dietary (10 K D₃) or systemic (DH D₃), in comparison to the vehicle-pretreated group. (b), Quantitation of cell death in A431 tumors after preconditioning with dietary or systemic D₃ followed by ALA-PDT. Note that the apoptosis-enhancing effect of dietary preconditioning is similar to that of systemic preconditioning. Mean \pm SEM from three images from each of five to nine tumors per treatment group; *P* values from unpaired two-sided *t*-test is shown above the brackets. (c), Tumor specificity of D₃ apoptotic enhancement. PDT-induced cell death in normal skin adjacent to the tumor was minimal, and very similar after pretreatment with D₃ or DH D₃ as after pretreatment with vehicle alone. *Dashed line*, basement membrane between dermis and epidermis. *Dotted line*, junction between stratum corneum (above) and viable epidermis (below). Scale bars 50 μm .

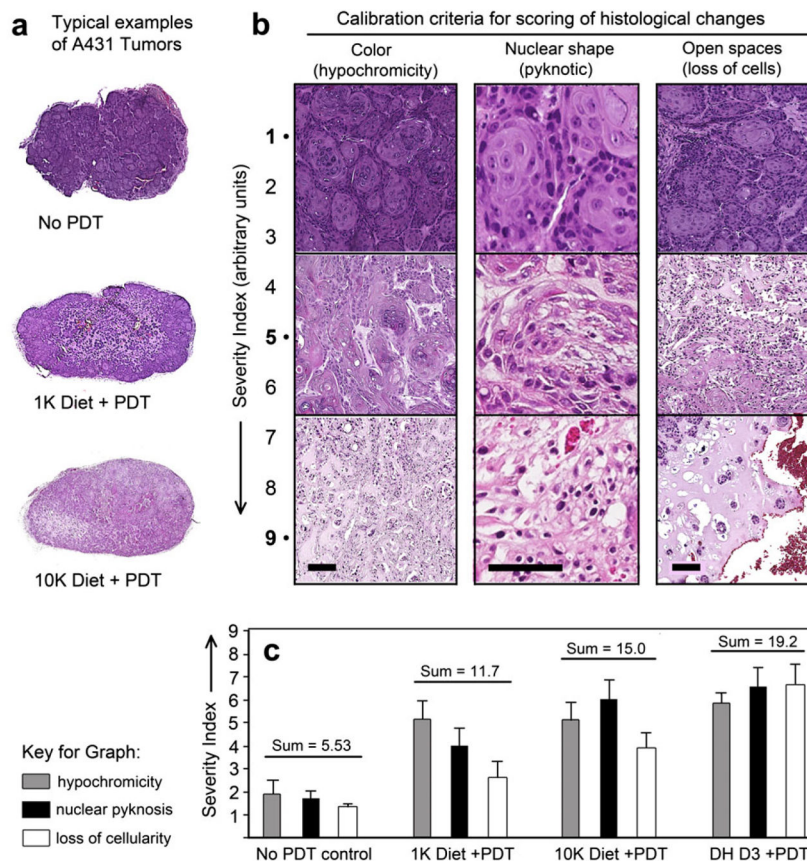


Figure 6.

Tumor morphology at 24 h post-PDT, with or without D₃ pretreatment. (a), H&E-stained images of whole A431 tumors, showing the overall effect of D₃ pretreatment upon the histological appearance after PDT-induced damage. (b), Magnified areas, showing examples of a 9-point scale (Severity Index) that was used to rate each tumor in these experiments, using three criteria: Loss of staining color (hypochromicity); shrinkage of nuclei (pyknosis); and open, cell-free zones (loss of cellularity). Scale bars, 50 μm. (c). Quantitation of cell death in tumors using the 9-point severity index. All specimens were scored by three independent observers, and the results pooled (mean ± SEM from three images each from six to eight tumors per treatment group). Note the increase in all three parameters following ALA-PDT and further increase after combination with Vit D₃ prior to ALA-PDT. The sum of all three parameters is shown above each experimental condition.

Table 1

Serum levels of Vit D₃ metabolic forms in mice following dietary or systemic treatment regimens

Vit D ₃ [metabolic form, dose]	Serum D ₃ (cholecalciferol) (ng mL ⁻¹)			Serum 25(OH)D ₃ (calcidiol) (ng mL ⁻¹)			Serum 1,25(OH) ₂ D ₃ (calcitriol) (pg mL ⁻¹)		
	Mean	Range	n	Mean	SD	n	Mean	SD	n
Oral delivery									
1 K [D ₃ , 1000 IU]	13.5	12.6	2	18.4	5.4	6	10.6	2.3	4
5 K [D ₃ , 5000 IU]	38.4	10.4	2	32	6.1	2	20.4	8.1	2
10 K [D ₃ , 10 000 IU]	41.3	2.7	2	41.3	10.4	4	21.1	9.5	4
Injected									
D ₃ [D ₃ , 1.25 µg kg ⁻¹]		ND		46.4	20.9	5	35.1	23.4	5
MH [25(OH) D ₃ , 250 µg kg ⁻¹]		ND		178	42.4	5	51.3	25.1	5
DH [1,25(OH) ₂ D ₃ , 1 µg kg ⁻¹]		ND		16.4	3.44	5	23.5	5.4	5

ND, not done.